frontiers in Physics

ORIGINAL RESEARCH
published: 28 March 2022
doi: 10.3389/fphy.2022.870339

Simulations and Experiments Toward Continuous Wave 167 nm Laser Generation for ARPES With High Energy Resolution

Ziyue Zhang[1,2], *Hainian Han*[1,3]*, *Guodong Zhao*[1], *Guodong Liu*[1], *Xingjiang Zhou*[1] and *Zhiyi Wei*[1,3]

[1]Beijing National Laboratory for Condensed Matter Physics, Institute of Physics, Chinese Academy of Sciences, Beijing, China, [2]Qian Xuesen Laboratory of Space Technology, China Academy of Space Technology, Beijing, China, [3]Songshan Lake Materials Laboratory, Dongguan, China

Continuous wave (CW) laser at a vacuum ultraviolet (VUV) range with the narrow-linewidth is an ideal optical source in angle-resolved photoemission spectroscopy (ARPES) for the research of superconductors with a narrow band gap. In this study, we present an eighth-harmonic-generation (EHG) laser scheme for CW laser generation at the VUV range, in particular at 167.75 nm, based on the cascaded power enhancement cavities. An intracavity second-harmonic generation (ICSHG) 671 nm laser with the narrow-linewidth and active frequency stabilization is built as the first stage, delivering the 2.55 W output power. A resonant cavity for fourth-harmonic-generation (FHG) constitutes the second stage, which generates the 335.5 nm laser with the output power of up to 1.25 W. The third stage is designed for the EHG of 167.75 nm based on the KBBF crystal. To realize the efficient CW laser generation at 167.75 nm, a theoretical analysis concerning the enhancement factor and the conversion efficiency of the KBBF-based EHG is carried out. The results show that it is possible for mW-level 167.75 nm generation if the transmittance of the KBBF prism-coupled device is increased to 97%. A 59 W circular intracavity power is observed in the 335.5 nm enhanced cavity experiments, corresponding to the peak power density of up to 20.86 MW/cm^2. This work paves a solid way for CW VUV laser generation with the narrow-linewidth, which would be an ideal tool for the extremely high resolution ARPES.

Keywords: vacuum ultraviolet, resonant enhancement, second-harmonic generation, narrow-linewidth, KBBF, ARPES

OPEN ACCESS

Edited by:
Xing Fu,
Tsinghua University, China

Reviewed by:
Zhigang Zhao,
Shandong University, China
Chaitanya Kumar Suddapalli,
The Institute of Photonic Sciences (ICFO), Spain

***Correspondence:**
Hainian Han
hnhan@iphy.ac.cn

Specialty section:
This article was submitted to Optics and Photonics, a section of the journal Frontiers in Physics

Received: *06 February 2022*
Accepted: *25 February 2022*
Published: *28 March 2022*

Citation:
Zhang Z, Han H, Zhao G, Liu G, Zhou X and Wei Z (2022) Simulations and Experiments Toward Continuous Wave 167 nm Laser Generation for ARPES With High Energy Resolution. Front. Phys. 10:870339. doi: 10.3389/fphy.2022.870339

INTRODUCTION

Angle-resolved photoemission spectroscopy (ARPES) is the most direct and powerful method to study the electronic structure of materials and plays an important role in the fields of advanced materials including high temperature superconductors, topological materials, and quantum materials. The higher the photon energy of the drive sources is, the larger the Brillouin zone can be measured, which is preferred for the research of superconductors with a narrow band gap. With the traditional vacuum ultraviolet (VUV) pulsed lasers as the drive sources, the energy resolution of the ARPES is limited to meV and the space charge effect affects the reliability of the

obtained spectroscopy. The narrow-linewidth continuous wave (CW) VUV lasers can be utilized as an alternative drive source to improve the energy resolution to neV and eliminate the space charge effect [1–6]. The narrow-linewidth continuous wave lasers have also revolutionized the fields of precision metrology through atomic and molecular spectroscopy. The 167.079 nm narrow-linewidth CW laser corresponds to the transition from $^1S_0$ to $^3P_0$ of $^{27}Al^+$, used for achieving the Doppler cooling of the aluminum ions optical clocks [7]. So it is important to develop > 7 eV VUV narrow-linewidth CW laser sources.

There are several methods to generate VUV lasers such as free electron lasers, high harmonic generation and synchrotron radiation, and so on, which are all pulsed lasers and very expensive scientific facilities [8–10]. The excimer lasers are the most common deep ultraviolet lasers, which are key elements in the fields of lithography. However, they are mostly pulsed lasers with a single repetition frequency and have a poor beam quality, which brings inconvenience to the scientific application [11]. The VUV generation based on nonlinear frequency conversion has attracted great attention because of the good beam quality, high compactness, high robustness, and the flexible parameter adjustability [12]. Several reports have classified the ultraviolet nonlinear crystals through the generated photon energy limit and absorption edge, showing that the $KBe_2BO_3F_2$ (KBBF) crystal is the only transparent medium supporting the > 7 eV second-harmonic generation (SHG) [13]. A number of ultraviolet laser results based on the KBBF nonlinear crystal have been reported including femtosecond, picosecond to quasi-CW microsecond pulse durations generation, joule to microjoule pulse energies generation, 170–210 nm tuning wavelengths generation, which have also been used to drive the ARPES, photoemission electron microscopy, and revolutionized many frontier research studies [14–18]. In 2015, S. B. Dai et al. demonstrated a 65 μW 167.75 nm picosecond pulse laser generation based on the eighth-harmonic generation (EHG) of the 1,342 nm picosecond fundamental frequency laser [19]. In 2018, J. J. Li et al. present the 1.5 μJ 167.79 nm laser output with the linewidth of 0.025 pm, which was also generated from EHG of a 5 Hz 1,336 nm fundamental frequency quasi-CW laser [20].

When it comes to VUV narrow-linewidth CW laser generation, the conversion efficiency of the single-pass nonlinear process such as SHG and sum-frequency generation is extremely low as the focused power density hardly reaches MW/cm^2. The resonant enhanced cavity is generally used to improve the SHG efficiency of the CW lasers. However, it is still difficult to generate VUV through cavity-enhanced SHG based on the KBBF nonlinear medium. There are three main obstacles: first, the loss of the ultraviolet resonant cavity is hard to control, which mainly comes from the unmature ultraviolet coating technology and the complex structure of the KBBF prism-coupled device (KBBF-PCD) [21]. The former limits the reflectivity and adds the transmission loss of the cavity mirrors. Every time passing through the KBBF-PCD, the laser beam suffers the Fresnel reflection loss, unpredictable scattering, and absorption losses due to the uneven optical-contact interface, making it difficult to enhance the fundamental laser. Second, the fundamental ultraviolet output power is also much lower than the common visible and near-infrared wavelength and there are few commercial products. Third, cascading resonant cavities with the Pound–Drever–Hall (PDH) techniques make it challenging to keep the compactness and long-term operation [22]. In 2012, M. Scholz et al. reported a 1.3 mW 191 nm VUV laser generated from the fourth-harmonic generation (FHG) of a commercial 764 nm semiconductor laser with the power of 1.6 W and the line width of 50 kHz [23]. In 2013, they utilized 3 W 772 nm semiconductor lasers as the fundamental source and generated the 193 nm CW VUV laser with the stable output power of 4 mW [24].

In this report, we present the theoretical and experimental results ready for the 167.75 nm VUV CW laser generation. A narrow-linewidth Nd: YVO_4 single-frequency CW laser based on the intracavity second-harmonic generation (ICSHG) is utilized as the fundamental source with the output power of 2.55 W at 671 nm. The active frequency stabilization is built to suppress the frequency jitter. The second cavity-enhanced FHG stage is based on a BBO crystal, delivering a 1.25 W 335.5 nm laser. The third SHG stage is designed to employ the KBBF crystal. A theoretical analysis is carried out, showing that the prerequisite of the mW-level 167.75 nm VUV CW laser generation is the transmittance of the KBBF-PCD increased to more than 97%. A 59 W circular intracavity power of the 335.5 nm is experimentally observed in the resonant EHG cavity, laying a good foundation for the 167.75 nm VUV CW laser generation.

LASER SYSTEMS FOR 335.5 NM GENERATION

A high power all-solid-state single-frequency CW laser with the active frequency stabilization system is used as the fundamental source, as shown in **Figure 1**. An 880 nm laser diode is used to pump the Nd: YVO_4 gain medium, and a TGG device is inserted to keep the direction of optical beam. An LBO nonlinear crystal is placed between the concave mirrors to convert the 1,342 nm radiation to the 671 nm laser, synchronously choosing the resonant wavelength and maintaining the sing-frequency operation [25]. The output power of the 671 nm laser is 2.55 W with a peak-to-peak variation of 0.69%, as shown in **Figure 2A**. The M^2 factor is measured to be 1.14 in the x direction and 1.09 in the y direction respectively, exhibiting a good beam quality.

To further suppress the short-term and long-term frequency drift, an active frequency stabilization system based on the Pound–Drever–Hall (PDH) method is built as shown in **Figure 1**. A 10 cm-long Fabry–Perot cavity made of indium steel material is chosen as the reference for the pre-stabilization stage. The leakage of the 1,342 nm single-frequency laser, the line width of which is measured to be 115 kHz, is led to the Fabry–Perot cavity after frequency was modulated using an electro-optic modulator (EOM). A photodetector is placed at the end of the Fabry–Perot cavity to get the transmitted signal, which is then demodulated in the phase detector and processed using a PID controller. The control

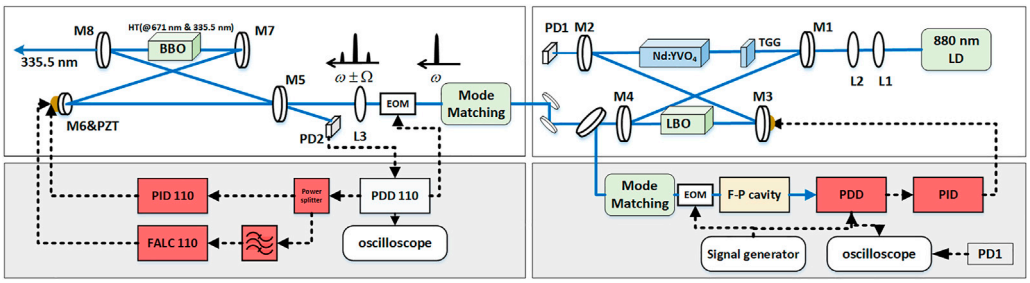

FIGURE 1 | Fourth harmonic laser system. M1–M8: cavity mirrors. L1-L3: focused lens. LD: Laser diode. EOM: Electro-optic modulator. PD: Photodiode.

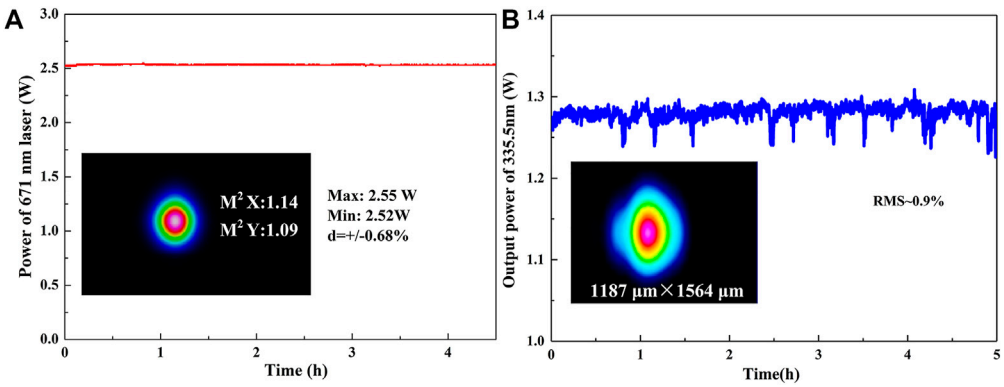

FIGURE 2 | (A) Stability of the output power of the 671 nm laser, the inset: beam quality. **(B)**The stability of the 335.5 nm single-frequency laser, the inset: the beam profile.

signal of the PID output is added to the piezo transducer (PZT) glued on the cavity mirror. The short-term frequency drift is suppressed from 100 MHz/2 min to less than 17.5 MHz/2 min, and the long-term frequency drift is suppressed by a factor of 2. The pre-stabilization cavity helped control the high frequency noise of the 671 nm single-frequency laser, benefiting the locking state of the cascading resonant cavity stages.

The second stage is designed to generate the fourth harmonic of the 1,342 nm single-frequency radiation. A 671 nm resonant cavity based on the nonlinear BBO crystal is built with the PDH locking system. After proper mode matching, the 2.55 W 671 nm laser is injected into the bow-tie resonant cavity with a conversion efficiency of 49%. The output power of the 335.5 nm ultraviolet laser is 1.25 W with a rms variation of 0.9% within 5 h because of the environmental disturbances, as shown in **Figure 2B**. Due to the walk-off effect, the beam spot of the 335.5 nm laser is elliptical even after being shaped by the cylindrical mirror, as shown in **Figure 2B**, bringing trouble to the mode matching of the next resonant stage. We estimate the line width of the second-harmonic at 671 nm to be < 163 kHz and the linewidth of the fourth-harmonic at 335.5 nm to be 230 kHz, as the SHG process increase the spectral linewidth with a factor of $\sqrt{2}$ [23].

VUV LASER GENERATION

Theoretical Background

According to the theory of G. D. Boyd, D. A. Kleiman, and A. Ashikin, when the fundamental frequency laser passes through a nonlinear crystal in a phase-matched direction, the output power P_2 of the SHG is as follows:

$$P_2 = E_{SHG} \cdot P_1^2, \tag{1}$$

where P_1 is the power of the fundamental frequency laser [26–28]. The nonlinear efficiency E_{SHG} is written as follows:

$$E_{SHG} = \frac{2\omega_1^2 d_{eff}^2}{\pi \varepsilon_0 c^3 n_1^2 n_2} \cdot lk_1 e^{-\alpha' l} \cdot h, \tag{2}$$

where ω_1 and k_1 are the angular frequency and wave vector of the fundamental frequency respectively, n_1 and n_2 are the indices of refraction of the fundamental frequency and the second harmonic respectively, d_{eff} is the effective nonlinear coefficient at the fundamental frequency, and l is the optical path in the nonlinear medium. $\alpha' = \alpha^1 + 1/2\alpha^2$, where α^1 and α^2 are the absorption coefficient for the fundamental and second harmonic respectively. The function h is expressed as follows:

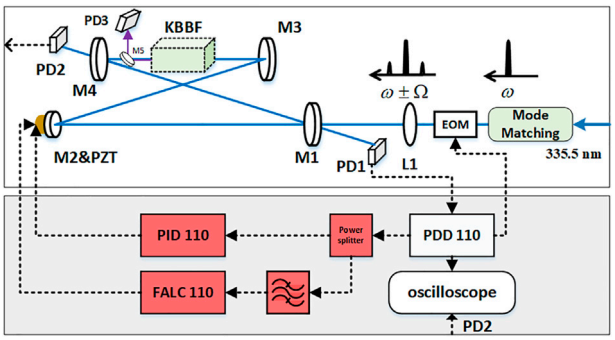

FIGURE 3 | Experimental setup of the resonant cavity based on the KBBF crystal. M1-M5: cavity mirror, PD: Photodetector, PZT: Piezo electric transducer, EOM: electronic-optical modulator.

$$h = \frac{\pi^2}{\xi_x} exp(\mu\alpha l)\left[\frac{2}{\sqrt{\pi}} e \int_{-\infty}^{\infty} exp(-4s^2)|H|^2 ds\right]. \quad (3)$$

According to Ref. [28], where $\xi_x = \frac{l}{b_x} = \frac{l}{k_1\omega_x^2}$ is the focusing parameter and

$$H = \frac{1}{2\pi} \int_{-\xi_x(1-\mu)}^{\xi_x(1+\mu)} \frac{exp(-\kappa\tau_x') exp(i\sigma'\tau_x')}{(1+i\tau_x')^{\frac{1}{2}}[1+i(e^2\tau_x'+\Delta)]^{\frac{1}{2}}} d\tau_x'. \quad (4)$$

The focus position is $\mu = \frac{l-2f_x}{l}$, and the astigmatic distance beam waists are $\Delta = \frac{2(f_x-f_y)}{k_1\omega_y^2}$. The ellipticity of the Gaussian beam is $e = \frac{\omega_x}{\omega_y}$, and the phase mismatch is $\sigma' = 1/2\, k_1\omega_y^2\Delta k + 4s\rho\omega_x k_1/2$. $\kappa = 1/2(\alpha^1 - 1/2\alpha^2)k_1\omega_x^2$.

Since the nonlinear efficiency of a type-I phase-matched crystal is low and the fundamental power of a CW laser is not comparable with high-peak-power narrow-duration pulsed lasers, the output power of the single-pass nonlinear process is usually at less than μW-level. A bow-tie resonant cavity is designed to enhance the fundamental power and improve the SHG conversion efficiency, as shown in **Figure 3**. Mirror M1 and M2 are plane. The former is the input coupler with the reflectivity of r_1 and the transmission of t_1 corresponding to the fundamental frequency, and the latter is mounted on two PZTs to stabilize the cavity length to the resonant wavelength. The mirror M3 and M4 are concave and the nonlinear crystal is placed at the focus between them. The reflectivity of the mirror M2–M4 is assumed as r_2, r_3, and r_4. The mirror M4 is usually chosen as the output coupler of the second harmonic, but for the > 7 eV VUV lasers present coating technology can hardly maintain the high reflectivity of the fundamental frequency and high transmission of the second harmonic synchronously. As a result, a reflective output coupler is inserted with high transmission of fundamental laser and high reflection for the harmonic generation with a transmission of t_5. The KBBF-PCD is the nonlinear medium as mentioned before with a transmission of t_{PCD}.

When the fundamental laser is coupled into the cavity and circling around, the main losses it suffered are the transmission and scattering loss of cavity mirrors r_i, the transmission loss of the KBBF-PCD ($1\text{-}t_{PCD}$), and the nonlinear conversion loss ($1-t_{SHG}$). Therefore, the equivalent reflectivity of resonator cavity can be expressed as $\mathbf{r} = r_2r_3r_4t_5 \cdot t_{PCD} \cdot t_{SHG}$, and $t_{SHG} = 1 - E_{SHG} \cdot P_c$. As the resonant cavity enters a steady state, the incident fundamental power P_1, the reflected power of the input coupler P_r, and the total circulating power P_c in the cavity have the following relationship

TABLE 1 | Parameters related to the KBBF crystal.

Crystal length	1 mm
Phase-matching angle (335.5–167.75 nm)	73.2°
n_1 (335.5 nm in the KBBF)	1.5007
n_2 (167.75 nm in the KBBF)	1.4993
d_{eff} (335.5 nm in the KBBF)	0.14 pm/V
α_1	0.1 cm^{-1}
α_2	10 cm^{-1}
Walk-off angle	38.83 mrad

$$\frac{P_r}{P_1} = \frac{\left(\sqrt{r_1} - \sqrt{r}\right)^2}{\left(1 - \sqrt{r_1 r}\right)^2}, \quad (5)$$

$$\frac{P_c}{P_1} = \frac{t_1}{\left[1 - \sqrt{r_1 r}\right]^2} = \frac{t_1}{\left[1 - \sqrt{r_1 \cdot r_2r_3r_4t_5 \cdot t_{PCD} \cdot (1 - E_{nl} \cdot P_c}\right]^2}, \quad (6)$$

when the reflectivity of the input coupler is consistent with the equivalent reflectivity of the cavity, $r_1 = r$, the impedance matching is fulfilled, which means the most efficient input coupling of the fundamental laser.

Simulation Results

The cavity is designed as shown in **Figure 3**. The reflectivity of the cavity mirrors M2–M4 is designed as $r_2 = r_3 = r_4 > 99.8\%$ at 335.5 nm, which is the highest reflectivity present coating technology can get. The output coupler M5 is designed as $t_5 > 99.5\%$ at 335.5 nm and $r_5 > 94\%$ at 167.75 nm. The parameters related to the KBBF device are listed in **Table 1**. The conversion efficiency is E_{SHG} calculated to be 1.41×10^{-6}/W.

Assuming that the mirrors are ideal and the input beam of the fundamental laser is circular and optimal mode matching, the input power of the fundamental laser is about 1.1 W. According to **Eqs 1–6**, simulations of the resonant cavity is carried out and the results are shown in **Figure 4**.

First, when the transmittance of the KBBF device is determined, the intracavity circulating power varies with the reflectivity of the input coupler and there is an optimum corresponding to the impedance matching state. For instance, when $t_{PCD} = 99\%$, the impedance matching appears at $r_1 = 97.9\%$. In this condition, the intracavity power P_c of the fundamental 335.5 nm laser is 52.58 W and the generated harmonic 167.75 nm is 3.89 mW theoretically, the nonlinear efficiency of which is only 0.35%.

Second, as the transmittance of the KBBF-PCD decreases from 99% to 97%, the optimal intracavity circulating power also decreases significantly from 52.58 W to 25.06 W and the impedance matching reflectance of the input coupler drops from 97.9% to 95.9%. The theoretically generated harmonic laser drops from 3.89 mW to 1.03 mW and the nonlinear

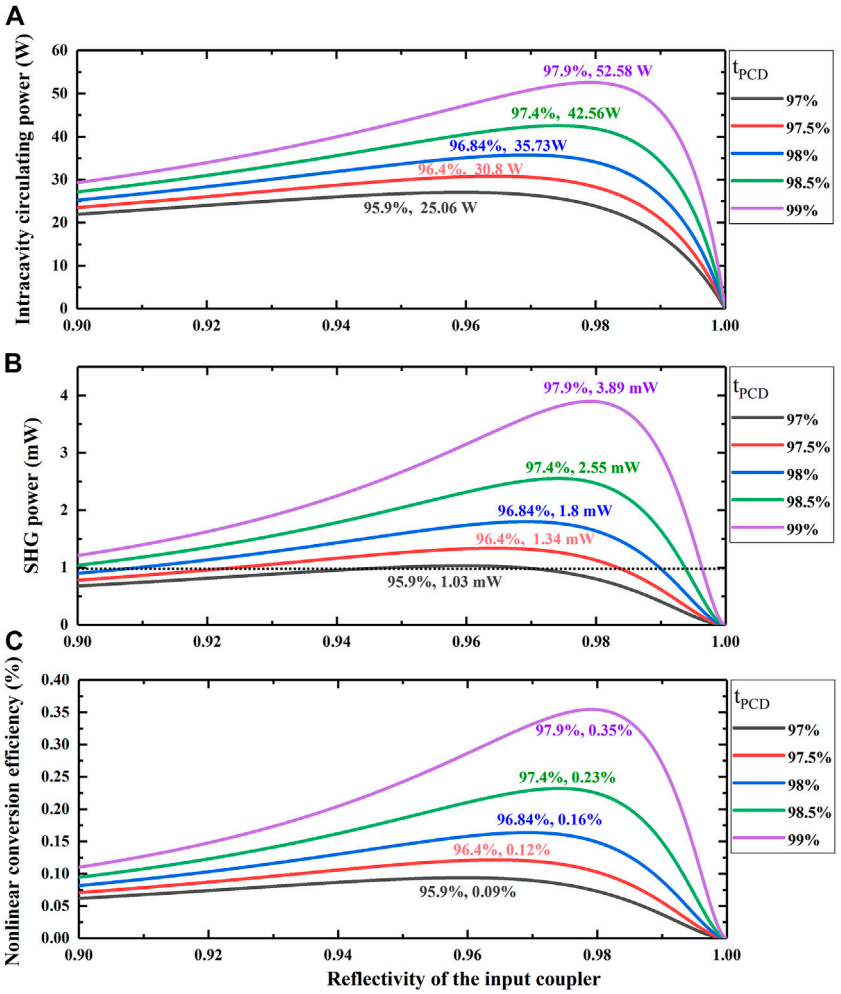

FIGURE 4 | (A) Intracavity circular power, **(B)**second-harmonic generation output power, and **(C)** nonlinear conversion efficiency versus input coupler.

conversion efficiency reduces from 0.35% to less than 0.09%, indicating that the transmittance of the KBBF-PCD is the key factor for the generation of the 167.75 nm harmonic laser. As the KBBF crystal is difficult to grow in the z-direction and cannot be cut along the phase-matching angle, a PCD structure was invented by C. T. Chen et al. to fix the crystal between prisms. The inhomogeneous optical contact introduces scattering loss at the interfaces of the KBBF medium and prims. The large phase-matched angle 73.2° makes the Fresnel reflection loss larger than 12%. These technical problems make it very challenging to control the transmission loss of 335.5 nm fundamental laser passing through a phase-matched KBBF-PCD less than 3%, which is predicted as the prerequisite for the generation of mW-level of the 167.75 nm VUV CW single-frequency laser.

Experimental Results

A bow-tie resonant EHG cavity is built according to the previous calculations and designs as shown in **Figure 3**. Since the VUV laser is absorbed seriously by the oxygen in the air, the whole cavity is built in a large vacuum chamber.

The distance S1 between plane mirror M1 and M2 is about 120 mm, and the beam waist between the plane mirror M1 and M2 is calculated to be 185 μm. The radius of the concave mirrors is 100 mm and the distance between them is adjusted to be 115 mm. The total length of the cavity is 493 mm. The reflectivity of the input coupler is designed to be 97%, and the others are 99.8% reflective. In order to efficiently couple the fundamental laser into the EHG resonant cavity, mode matching of the fundamental laser with the resonant mode is of great importance. As a result, after changing different groups of lenses, we chose a lens with the focal length of 1-m to shape the fundamental laser to $173 \times 207\,\mu m^2$, which is the optimal mode-matching conditions as the walk-off effect leading to an elliptical beam spot.

In order to achieve the PDH stabilization, two PZTs with the displacement of 2 μm and 10 μm were used for the fast-loop and slow-loop stabilization respectively. The size of the plane mirror M2 is $\phi 6 \times 2\,mm^2$ to reduce the load of the PZTs. A photodetector PD1 is placed behind the input coupler M1 to detect the reflective signal. Another photodetector PD2 is placed

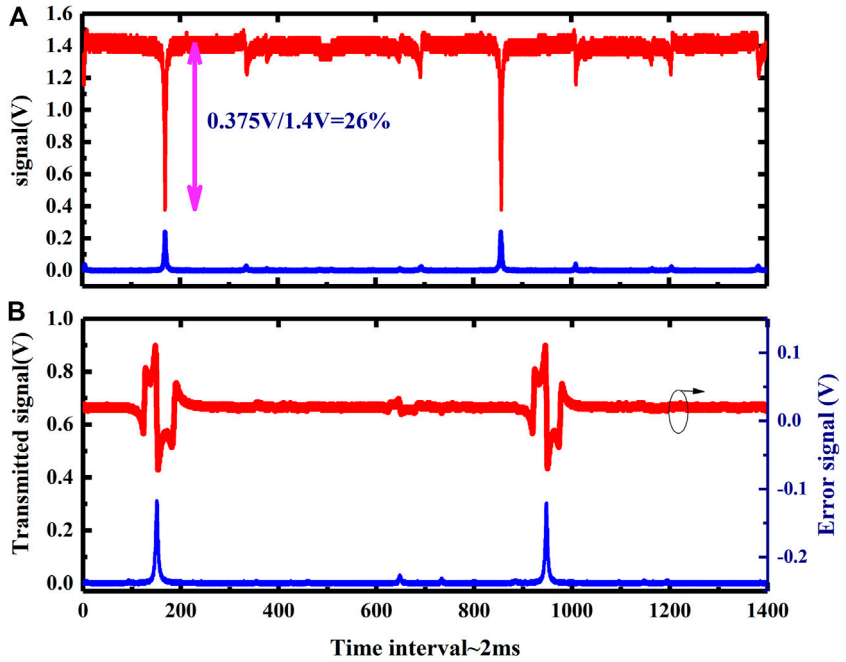

FIGURE 5 | (A) Reflection peaks (red) and transmission peaks (blue) of the 335.5 nm resonant cavity; **(B)** error signals (red).

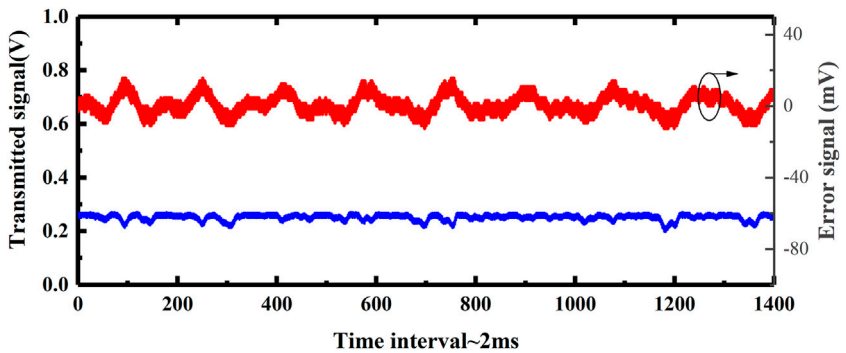

FIGURE 6 | Transmitted signal (blue) and error signal (red) of the PDH locked resonant cavity.

behind the concave mirror to detect the leakage. The locking electronics are from Toptica electronics.

The laser is first phase modulated using an EOM with the modulation frequency of 20 MHz, the detected reflected signal and transmitted signal are shown in **Figure 5A**. The positions of the focusing lens and the cavity mirrors are carefully adjusted according to the detected signals to suppress the high-order modes and improve the amplitude of the circulating power. The reflected signal is optimized as shown in **Figure 5A**, about 26% power was reflected at the resonant position, which is attributed to the mode mismatching and the impedance mismatching.

The reflected signal is then demodulated by the phase detector and the error signal is shown in **Figure 5B**. Two PID modules also from Toptica electronics are used to stabilize the cavity to the resonant wavelength. Once the locking state is activated, the error signal becomes zero and the transmitted signal stays at the high level, as shown in **Figure 6**. The leakage power of the concave mirror with a transmittance of 0.206% is measured to be 121 mW, and the circulating intracavity power is inferred to be 59 W. According to **Eq. 6**, under certain conditions the reflectivity of the input coupling is 97%, then the enhanced factor would be 90. The difference is attributed to the unperfect mode mismatching and the other scattering losses.

CONCLUSION

We have demonstrated the generation of the 335.5 nm laser with a high-peak-power density ready for the generation of the

narrow-linewidth 167.75 nm VUV single-frequency CW laser, based on a home-built resonant cavity. The cascading resonant harmonic generation systems are designed, delivering the 671 nm single-frequency CW laser with the output power of the 2.55 W and the 335.5 nm single-frequency of 1.25 W. The EHG resonant cavity is preliminarily verified with the circulating power of 59 W and the peak power density of 20.86 MW/cm^2. A theoretical analysis is carried out, indicating that improving the transmittance of the KBBF-PCD to larger than 97% is the prerequisite for the mW-level generation of the 167.75 nm VUV narrow-line width single-frequency CW laser.

DATA AVAILABILITY STATEMENT

The raw data supporting the conclusion of this article will be made available by the authors, without undue reservation.

AUTHOR CONTRIBUTIONS

GL and XZ contributed to the ARPES application requirements. ZZ, HH and ZW contributed to the design and experimental schemes. ZZ and HH performed the experiments and are responsible for the data processing. ZZ, GZ, HH, and ZW contributed to write and edit the manuscript.

FUNDING

This work was supported by the Strategic Priority Research Program of the Chinese Academy of Sciences (Grant Nos. XDA1502040404 and XDB25000000) and the National Natural Science Foundation of China (Grant Nos. 91850209, 11888101 and 11974404).

REFERENCES

1. Zhou XJ, Wannberg B, Yang WL, Brouet V, Sun Z, Douglas JF, et al. Space Charge Effect and Mirror Charge Effect in Photoemission Spectroscopy. *J Electron Spectrosc Relat Phenomena* (2005) 142(Issue 1):27–38. ISSN 0368-2048. doi:10.1016/j.elspec.2004.08.004
2. Zhou XJ, Cuk T, Devereaux T, Nagaosa N, Shen Z-X. Angle-Resolved Photoemission Spectroscopy on Electronic Structure and Lectron-Phonon Coupling in Cuprate Superconductors. In: JR Schrieffer JS Brooks, editors. *Handbook of High-Temperature Superconductivity*. New York, NY: Springer (2007). p. 87–144. doi:10.1007/978-0-387-68734-6_3
3. Damascelli A, Hussain Z, Shen Z-X. Angle-resolved Photoemission Studies of the Cuprate Superconductors. *Rev Mod Phys* (2003) 75:473–541. doi:10.1103/RevModPhys.75.473
4. Tamai A, Meevasana W, King PDC, Nicholson CW, de la Torre A, Rozbicki E, et al. Spin-orbit Splitting of the Shockley Surface State on Cu(111). *Phys Rev B* (2013) 87:075113. doi:10.1103/PhysRevB.87.075113
5. Taniuchi T, Kotani Y, Shin S. Ultrahigh-spatial-resolution Chemical and Magnetic Imaging by Laser-Based Photoemission Electron Microscopy. *Rev Scientific Instr* (2015) 86:023701. doi:10.1063/1.4906755
6. Tamai A, Wu QS, Cucchi I, Bruno FY, Riccò S, Kim TK, et al. Fermi Arcs and Their Topological Character in the Candidate Type-II Weyl SemimetalMoTe2. *Phys Rev X* (2016) 6:031021. doi:10.1103/PhysRevX.6.031021
7. Chou CW, Hume DB, Koelemeij JC, Wineland DJ, Rosenband T. Frequency Comparison of Two High-Accuracy Al+ Optical Clocks. *Phys Rev Lett* (2010) 104:070802. doi:10.1103/PhysRevLett.104.070802
8. O'Shea P, Freund H Free-Electron Lasers: Status and Applications. *Science* (2001) 292:1853–8. doi:10.1126/science.1055718
9. Paul PM, Toma ES, Breger P, Mullot G, Auge´ F, Balcou P, et al. Observation of a Train of Attosecond Pulses from High Harmonic Generation. *Science* (2001) 292:1689–92. doi:10.1126/science.1059413
10. Moser HO, Wilhelmi O, Yang P Synchrotron Radiation Research At Singapore Synchrotron Light Source. *Accel. Phys. Technol. App.* (2004):601–627.
11. Basting D, Marowsky G. *Excimer Laser Technology*. Berlin, Heidelberg: Springer Berlin Heidelberg (2005). Imprint: Springer.
12. Peng Q-J, Zong N, Zhang S-J, Wang Z-M, Yang F, Zhang F-F, et al. DUV/VUV All-Solid-State Lasers: Twenty Years of Progress and the Future. *IEEE J Select Top Quan Electron.* (2018) 24(5):1–12. Art no. 1602312. doi:10.1109/JSTQE.2018.2829665
13. Liu G, Wang G, Zhu Y, Zhang H, Zhang G, Wang X, et al. Development of a Vacuum Ultraviolet Laser-Based Angle-Resolved Photoemission System with a Superhigh Energy Resolution Better Than 1 meV. *Rev Sci Instrum* (2008) 79:023105. doi:10.1063/1.2835901
14. Yang F, Wang Z, Zhou Y, Li F, Xu J, Xu Y, et al. Theoretical and Experimental Investigations of Nanosecond 177.3 Nm Deep-Ultraviolet Light by Second Harmonic Generation in KBBF. *Appl Phys B* (2009) 96:415–22. doi:10.1007/s00340-009-3506-z
15. Yang F, Wang Z, Zhou Y, Cheng X, Xie S, Peng Q, et al. 41mW High Average Power Picosecond 177.3nm Laser by Second-Harmonic Generation in KBBF. *Opt Commun* (2010) 283:142–5. doi:10.1016/j.optcom.2009.09.051
16. Wang G, Wang X, Zhou Y, Li C, Zhu Y, Xu Z, et al. High-efficiency Frequency Conversion in Deep Ultraviolet with a KBe_2BO_3F_2 Prism-Coupled Device. *Appl Opt* (2008) 47:486–8. doi:10.1364/ao.47.000486
17. Zhang H, Wang G, Guo L, Geng A, Bo Y, Cui D, et al. 175 to 210 Nm Widely Tunable Deep-Ultraviolet Light Generation Based on KBBF crystal. *Appl Phys B* (2008) 93:323–6. doi:10.1007/s00340-008-3198-9
18. Zhang X, Wang L, Wang X, Wang G, Zhu Y, Chen C. High-Power Sixth-Harmonic Generation of an Nd:YAG Laser with KBe2BO3F2 Prism-Coupled Devices. *Opt Commun* (2012) 285:4519–22. doi:10.1016/j.optcom.2012.06.080
19. Dai SB, Zong N, Yang F, Zhang SJ, Wang ZM, Zhang FF, et al. 167.75-nm Vacuum-Ultraviolet Ps Laser by Eighth-Harmonic Generation of a 1342-nm Nd:YVO_4 Amplifier in KBBF. *Opt Lett* (2015) 40:3268–71. doi:10.1364/OL.40.003268
20. Dai S-B, Chen M, Zhang S-J, Wang Z-M, Zhang F-F, Yang F, et al. 2.14 mW Deep-Ultraviolet Laser at 165 Nm by Eighth-Harmonic Generation of a 1319 Nm Nd:YAG Laser in KBBF. *Laser Phys Lett* (2016) 13:035401. doi:10.1088/1612-2011/13/3/035401
21. Chen CT, Wang GL, Wang XY, Xu ZY. Deep-UV Nonlinear Optical crystal KBe2BO3F2-Discovery, Growth, Optical Properties and Applications. *Appl Phys B* (2009) 97:9–25. doi:10.1007/s00340-009-3554-4
22. Black ED. An Introduction to Pound-Drever-Hall Laser Frequency Stabilization. *Am J Phys* (2001) 69:79–87. doi:10.1119/1.1286663
23. Scholz M, Opalevs D, Leisching P, Kaenders W, Wang G, Wang X, et al. 13-mW Tunable and Narrow-Band Continuous-Wave Light Source at 191 Nm. *Opt Express* (2012) 20:18659–64. doi:10.1364/oe.20.018659
24. Scholz M, Opalevs D, Leisching P, Kaenders W, Wang G, Wang X, et al. A Bright Continuous-Wave Laser Source at 193 Nm. *Appl.Phys Lett* (2013) 103:051114. doi:10.1063/1.4817786

25. Ma Y, Li Y, Feng J, Zhang K. High-power Stable Continuous-Wave Single-Longitudinal-Mode Nd:YVO_4 Laser at 1342 Nm. *Opt Express* (2018) 26: 1538–46. doi:10.1364/oe.26.001538
26. Ashkin A, Boyd G, Dziedzic J. Resonant Optical Second Harmonic Generation and Mixing. *IEEE J Quan Electron.* (1966) 2:109–24. doi:10.1109/jqe.1966.1074007
27. Boyd GD, Kleinman DA. Parametric Interaction of Focused Gaussian Light Beams. *J Appl Phys* (1968) 39:3597–639. doi:10.1063/1.1656831
28. Freegarde T, Coutts J, Walz J, Leibfried D, Hänsch TW. General Analysis of Type I Second-Harmonic Generation with Elliptical Gaussian Beams. *J Opt Soc Am B* (1997) 14:2010. doi:10.1364/josab.14.002010

Conflict of Interest: The authors declare that the research was conducted in the absence of any commercial or financial relationships that could be construed as a potential conflict of interest.

Publisher's Note: All claims expressed in this article are solely those of the authors and do not necessarily represent those of their affiliated organizations, or those of the publisher, the editors, and the reviewers. Any product that may be evaluated in this article, or claim that may be made by its manufacturer, is not guaranteed or endorsed by the publisher.